Hindawi Publishing Corporation
Journal of Nanomaterials
Volume 2015, Article ID 160212, 8 pages
http://dx.doi.org/10.1155/2015/160212

Research Article

Photocatalytic Oxidation of Trichloroethylene in Water Using a Porous Ball of Nano-ZnO and Nanoclay Composite

Sol-A Bak,[1] Myong-Shin Song,[1] In-Tak Nam,[2] and Woong-Geol Lee[3]

[1]*Research Center of Advanced Convergence Processing on Materials, Kangwon National University, Samcheok 245711, Republic of Korea*
[2]*Department of Nano Applied Engineering, Kangwon National University, Chuncheon 200701, Republic of Korea*
[3]*SPM Co., Ltd., Kangwon 220841, Republic of Korea*

Correspondence should be addressed to Myong-Shin Song; msong0422@kangwon.ac.kr and In-Tak Nam; itnam@kangwon.ac.kr

Received 1 May 2015; Accepted 30 August 2015

Academic Editor: Xiao-Miao Feng

The presence of nondegradable organic compounds and xenobiotic chemicals in water is a great concern for the general public because of their polar properties and toxicity. For instance, trichloroethylene (TCE) is a widely used solvent in the chemical industry, and it is also a contaminant of soil, surface water, and groundwater. Recent studies on new treatment technologies have shown that photocatalyst-based advanced oxidation processes are appropriate for removing these polar and toxic compounds from water. The objective of this study was to remove TCE from water using novel nano-ZnO-laponite porous balls prepared from photocatalyst ZnO with nanoscale laponite. These nano-ZnO-laponite porous balls have a porosity of approximately 20%. A lower initial concentration of TCE resulted in high removal efficiency. Moreover, the removal efficiency increased with increasing pH in the photocatalytic degradation experiments employing UVC light with nano-ZnO-laponite. The optimal dosage of nano-ZnO-laponite was 30 g and the use of UVC light resulted in a higher removal efficiency than that achieved with UVA light. In addition, the removal efficiency of TCE significantly increased with increasing light intensity. We think that TCE's removal in water by using porous ball of nano-ZnO and nanoclay composite is a result of degradation from hydroxide by photons of nano-ZnO and physical absorption in nanoclay.

1. Introduction

Rapid urbanization and industrialization have resulted in large-scale emission of organic compounds that do not occur naturally, which has led to serious environmental pollution. Many organic compounds are synthesized by ongoing developments and applications of the chemical industry, and a majority of the synthetic organic compounds are nondegradable, which means that they can be degraded neither naturally nor by biological treatment, including activated sludge. Many of these nondegradable organic compounds remain in nature for long periods, not only damaging the ecosystem but also threatening public health when they come into human contact. Thus, there is an urgent need to eliminate such compounds. In particular, these substances are known as the leading factors of soil and underground-water contamination. The reality is that nondegradable organic compounds cannot be easily treated in existing sewage-disposal plants. Water-quality regulations for sewage-disposal and wastewater-disposal plants, like biochemical oxygen demand (BOD), chemical oxygen demand (COD), and limits for suspended solids (SS), are becoming more stringent, and it has been more difficult to meet the allowable emission standards by only treating degradable substances [1–5].

Analysis results for underground water, sampled from 25,000–140,000 sites annually in South Korea, indicate that the percentage of ground water polluted by trichloroethylene (TCE), which exceeds the maximum defined in the quality standard for underground water, has increased: 15% in 2004, 16% in 2005, and 29% in 2006 [6–8]. A report from the Ministry of Environment (Korea) that provides measurements of underground water contamination indicates that, of the harmful substances exceeding the standards, the proportion of TCE was the highest and its contamination figures have not improved over the last four years. Moreover, the amount of

Table 1: Physical and chemical properties of ZnO.

Purity	Mean diameter (nm)	Specific surface ($m^2 \cdot g^{-1}$)	Dry loss (%)	Combustion loss (%)	Pb (%)	Cu (%)
99.7%	30	>90	<0.3	<0.2	≤0.037	≤0.0002

detected TCE was high in industrial complex areas and urban residential areas, demonstrating an urgent need for treatment of TCE-contaminated ground water [9, 10].

In this study, as an alternative to using TiO_2 for eliminating nondegradable organic compounds, the most commonly used photocatalyst, laponite, which has good photopermeability, was mixed with ZnO, which is known to be excellent at degrading TCE. The nano-ZnO-laponite complex was shaped into balls to increase the interface with TCE, and its TCE removal efficiency was then evaluated.

2. Experimental

2.1. Materials

2.1.1. ZnO-Laponite Composite. ZnO has attracted considerable interest because it has a wide band gap (3.37 eV) at room temperature and its electrical properties are improved by adding impurities and exposing the material to UV, or adding a luminous element in blue, since its exciton band energy is 60 meV. The nano-ZnO powder used in the experiments was purchased from SH Energy & Chemical, Korea, and the average particle diameter was 30 nm. Table 1 lists the general properties of ZnO. We used Laponite RD (Rockwood Additives Ltd., UK) as the photocatalyst. It is an inorganic protective powder with a disilicate structure (Figure 1) [11–14]. The general physical properties of laponite are listed in Table 2.

2.1.2. TCE. The TCE used in this study was a liquid product with a purity of 99.5% or higher, manufactured by Sigma-Aldrich in USA. It is a very volatile substance with a molecular weight of 131.39 g and a specific gravity of 1.465 $g \cdot cm^{-3}$. For our experiments, we prepared TCE with a concentration of 10 ppm.

2.1.3. NaOH and HCl. We used NaOH as an alkaline solvent and HCl as an acidic solvent to control the pH of TCE. The NaOH was 99.5% pure and a first-class reagent; the HCI was supplied by Tsurumi Soda (Japan).

2.2. Methods

2.2.1. Formation of Ball-Shaped Nano-ZnO-Laponite Composite. We formed the ZnO-laponite composite, the photocatalyst used in this study, into ball-shaped particles. The average size of each ball was about 3 mm. We prepared laponite by mixing it with water in a 1 : 10 (w/w) ratio with an agitator for 5 min, followed by drying at room temperature, resulting in a gel-state product. Another round of agitation was performed after mixing the gel laponite with nano-ZnO powder and adding a small amount of thickener. The mixing ratios of the gel laponite and nano-ZnO are listed in Table 3. We formed the mixed samples into ball shapes using a pill maker. The resulting nano-ZnO-laponite balls were dried in air for 48 h.

Table 2: Physical and chemical properties of laponite.

(a)

Physical property	
Powder color	White
Density ($kg \cdot m^{-3}$)	1000
Surface area ($m^2 \cdot g^{-1}$)	370
pH (2 wt% suspension)	9.8

(b)

Chemical composition (dry basis) (%)	
SiO_2	59.9
MgO	27.5
Li_2O	0.8
Na_2O	2.8
LOI*	8.2

*LOI = limiting oxygen index.

Table 3: Mixing proportions of nano-ZnO-laponite balls.

Type	Nano-ZnO (wt%)	Laponite (wt%)	Water (wt%)
1	90	10	10
2	88	12	10
3	86	14	10

2.2.2. Instrumentation. We used UVA and UVC lamps (Philips, Netherlands) in the experiments. The wavelengths of the UVA and UVC lamps were 360 and 254 nm, respectively. The respective specifications for the lamps are given in Table 4.

The reactor used in this study was custom-made. An illustration of the setup is shown in Figure 2, and the actual setting is shown in Figure 3. We inserted a quartz tube at the center and installed a UV lamp at each vertex of the reactor; the quartz tube was completely filled with the nano-ZnO-laponite composite. The walls of the reactor were acrylic. In addition, the exterior surface of the reactor was designed to prohibit the passage of light, while the interior surface had a mirrored coating. This setup offered the advantage of reusing the light source since the light could perform photocatalytic scanning after being reflected (without exiting the reactor).

2.2.3. Methods. The quartz tube was completely filled with the nano-ZnO-laponite composite (30 g), the photocatalyst used in the study. Then, the previously prepared TCE (60 mL), with a concentration of 10 $mg \cdot L^{-1}$, was added to

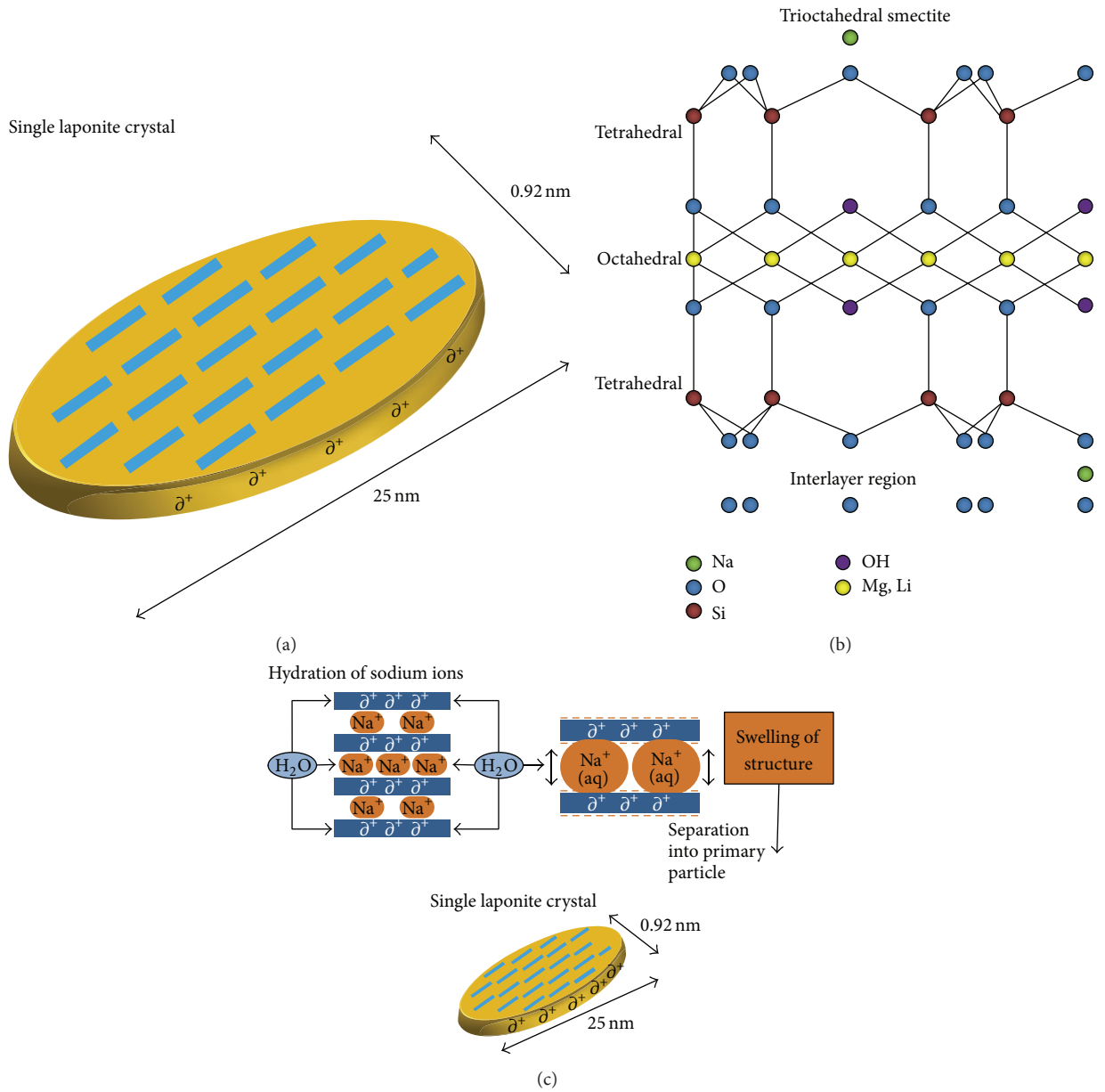

Figure 1: General properties of laponite: (a) single laponite crystal; (b) chemical structure of laponite; and (c) addition of laponite to water.

Table 4: Operating conditions for UVA and UVC.

Type	Power (W)	Dimensions (mm)		Lamp current (A)	Ultraviolet output (W)
		Length, L	Diameter, D		
TL8W/05 (UVA)	8	288.3	16	0.15	1.0
TUV 8W (UVC)	7	237.0	16	0.15	2.1

the quartz tube. The quartz tube was affixed inside the reactor with both ends sealed. The UV lamps were then turned on, and samples were collected at 30-minute intervals for 2 h. To induce instant deposition of the photocatalytic powder in the collected samples, we used a centrifugal separator. We checked the TCE removal efficiency by setting the changes in initial concentration, pH changes, lamp type, and the number of lamps (intensity of light) as variable factors.

2.2.4. Analysis. The analysis was using a purge-and-trap gas chromatograph (GC; 6890N, Agilent, USA) and mass spectrometer (MS) (purge-trap GC-MS) system. The operating conditions are as follows: the carrier gas, N_2 gas, entered at 1–5 mL·min^{-1}; the column temperature was 35–220°C, set at a heating/cooling rate of 10°C·min^{-1}; and the detector temperature was 230°C. We used a VOCOL (Sigma-Aldrich) capillary tube column. The activation conditions for the purge

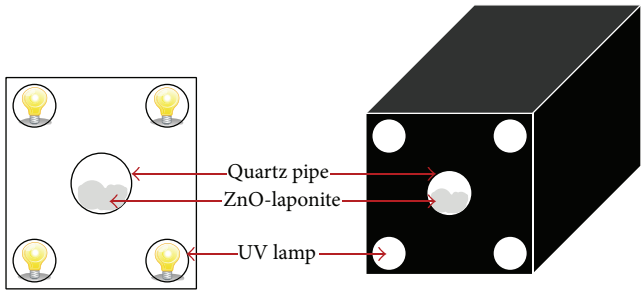

Figure 2: Scheme of the reactor.

Figure 3: Experimental setup of the reactor.

and trap devices are as follows: purge temperature = 30°C; purge time = 11 min; trap-bake temperature = 220°C; and trap-bake time = 7 min.

2.2.5. Measurement Methods of Removal Efficiency. Removal efficiency was measured as a percentage of removed concentration of TCE by injected initial concentration of TCE.

3. Results and Discussion

3.1. Properties of Nano-ZnO-Laponite Balls. The ZnO-laponite balls were ground into powder 48 h after formation, when they appeared to have strengthened. Figure 4 shows the X-ray diffraction (XRD) results for the powder to determine whether the ZnO crystals were altered by laponite. The peaks in the XRD pattern at 2θ values of 31, 34, 36, 47, 56, 62, and 67° can be assigned to specific peaks of ZnO. Therefore, we can conclude that the addition of laponite did not change the ZnO crystal structure. Figure 5 shows the results of the fine-structure analysis of the ZnO-laponite balls. This crystal analysis was carried out after cleaving through the surface and the central part of the ball, showing air gaps on the face and in the interior. Upon calculating the ratio of the cross-sectional areas, the air-gap ratio on the surface

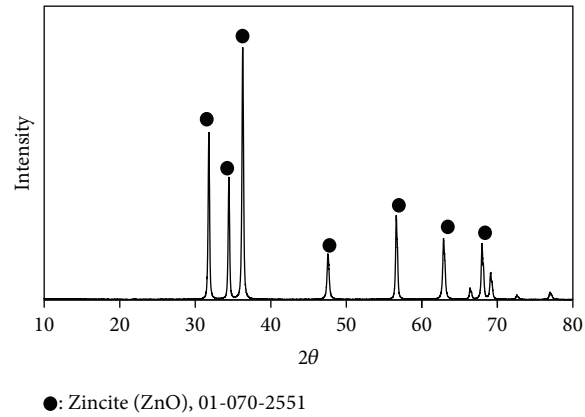

Figure 4: XRD results for a nano-ZnO-laponite ball.

was found to be about 20%; the air-gap ratio in the interior was almost the same. In other words, the overall air-gap ratio of a nano-ZnO-laponite ball was about 20%, which means that it was porous. Figure 6 shows the shape of the nano-ZnO-laponite balls, which were formed with uniform diameters of about 3 mm, with a formation strength of $5.0 \pm 0.5\ \text{N}\cdot\text{mm}^{-2}$ on average.

3.2. TCE Removal Using Nano-ZnO-Laponite

3.2.1. Changes in TCE Elimination by Varying the Initial TCE Concentration. Testing the correlation of the initial concentration of TCE in water with its susceptibility to the absorption and photocatalytic reaction is an important step in evaluating the process mechanisms and suitability of the treatment in field applications. Therefore, to measure the TCE removal ratio by the change from its initial concentration, we used initial concentrations of 1, 5, 10, and 20 $\text{mg}\cdot\text{L}^{-1}$; the pH was 7; the amount of added nano-ZnO-laponite was 30 g; and the reaction time was 60 min. Figure 7 shows the TCE removal ratios in terms of the initial concentration of source water (source water is defined as water in its natural state from streams, rivers, lakes, or underground aquifers, prior to any treatment).

Here, it can be seen that, after 40 min of reaction, the removal ratio was 99% or higher for an initial concentration of 1 $\text{mg}\cdot\text{L}^{-1}$ and about 55% for 20 $\text{mg}\cdot\text{L}^{-1}$. In other words, as the initial concentration of TCE decreased, the TCE removal ratio increased. This phenomenon indicates that with increasing initial concentration, more TCE particles were absorbed in the pores on the surface and interior of the nano-ZnO-laponite balls, which resulted in a dramatic reduction in the number of radical hydroxides ($^{\bullet}$OH) generated on the surface of each nano-ZnO-laponite ball by UV emission. The reduction in radical hydroxides, which have strong oxidizing power, decreased the removal ratio of TCE, which was degraded by the photocatalytic reaction [15, 16]. Furthermore, when the initial TCE concentration was high, the photons generated by UV emission were blocked by TCE particles in the liquid before they reached the surface of the nano-ZnO-laponite balls to stimulate the photocatalytic reaction.

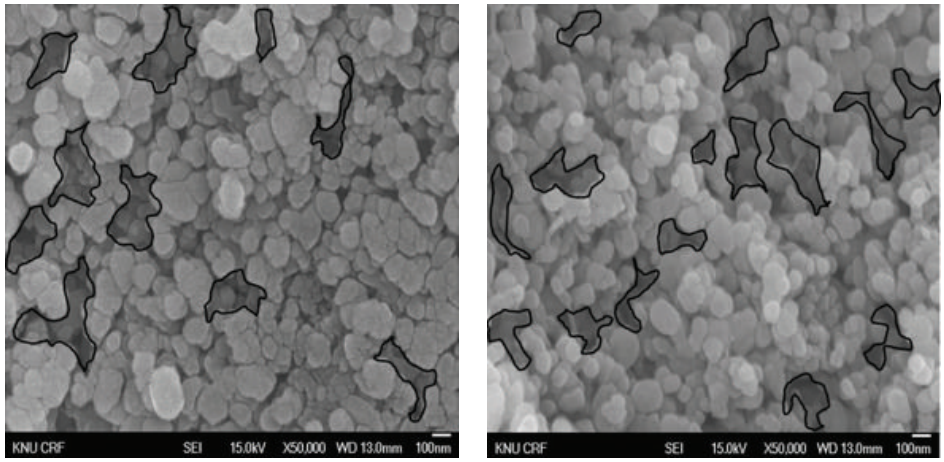

(a) (b)

Figure 5: SEM images of a nano-ZnO-laponite ball: (a) surface phase; (b) interior phase.

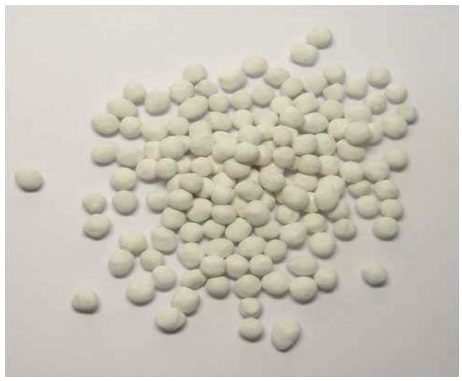

Figure 6: Shape of nano-ZnO-laponite balls.

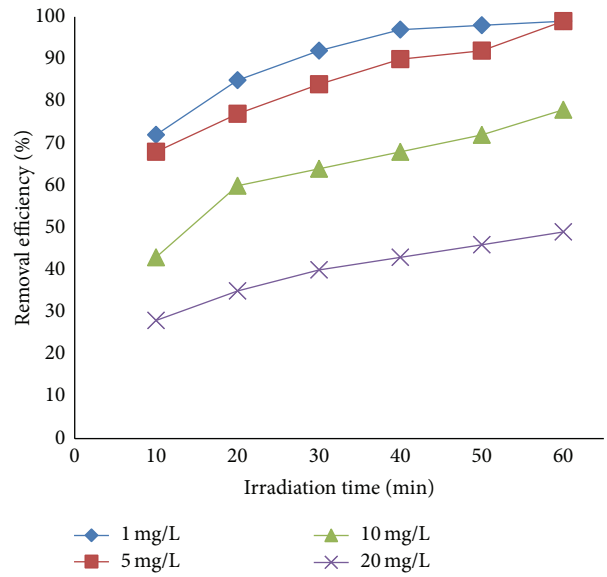

Figure 7: Effect of initial concentration of TCE on photocatalytic degradation (initial concentration of TCE = 1–20 mg·L^{-1}; nano-ZnO-laponite loading = 30 g; pH = 7.0; irradiation time = 60 min; and UVC intensity = 8.4 mW·cm^{-2}).

Therefore, the amount of photons absorbed on the surface of the nano-ZnO-laponite balls decreased, which also reduced the TCE removal ratio [17, 18]. Moreover, Carp et al., Yang et al., and Li et al. [17–19] reported that the reaction byproducts (intermediates) generated during the photocatalytic reaction also affect the TCE degradation rate; that is, source water with a high initial TCE concentration generates a large amount of reaction byproducts, resulting in an overall decrease in the TCE removal ratio.

3.2.2. TCE Removal Characteristics with respect to the Amount of Inserted Nano-ZnO-Laponite. We also examined how the amount of inserted nano-ZnO-laponite balls affected the absorption and photocatalytic reaction of TCE (Figure 8). The amounts of inserted nano-ZnO-laponite were 10, 20, 30, and 40 g. As this amount was gradually increased, the respective removal efficiencies were found to be 55.8, 71.5, 88.6, and 89.9%, indicating that the TCE removal ratio also increased continuously. This result was primarily due to the increase in the total surface area of nano-ZnO-laponite. A secondary factor for this behavior was that, as the active sites available for absorption and photocatalytic reaction were increased, large amounts of radical hydroxide and superoxide could be generated [17]. However, we only observed slight increases in the TCE removal ratio when the amount of inserted nano-ZnO-laponite was above 30 g. Thus, an unlimited increase of nano-ZnO-laponite balls did not continue to enhance the photocatalytic degradation. In other words, the economic reality and the effects of secondary environmental byproducts (byproducts generated after use) should be considered. In this regard, Choy and Chu [20] stated that the optimal catalyst loading should be selected to obtain optimal removal efficiency and economic efficiency.

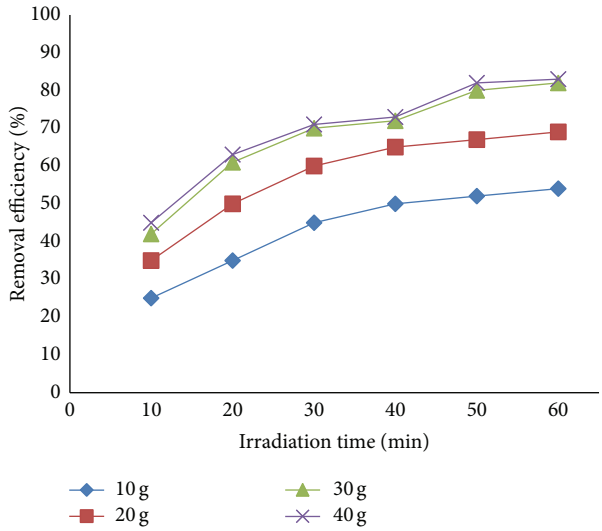

Figure 8: Effect of nano-ZnO-laponite loading on photocatalytic degradation (initial concentration of TCE = 10 mg·L^{-1}; nano-ZnO-laponite loading = 10–40 g; pH = 7.0; irradiation time = 60 min; and UVC intensity = 8.4 mW·cm^{-2}).

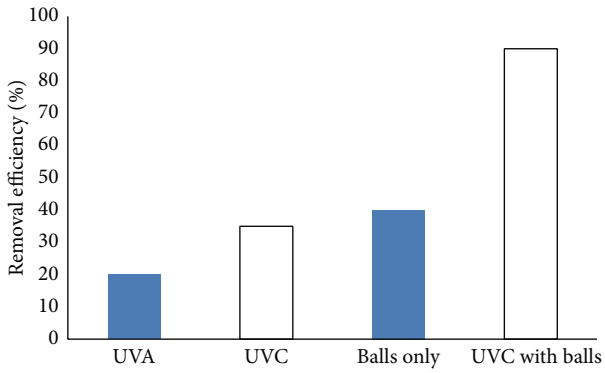

Figure 9: Removal efficiency by photolysis, adsorption, and photocatalysis of TCE with UVA or UVC, nano-ZnO-laponite balls only, and UVC with nano-ZnO-laponite balls (initial concentration of TCE = 10 mg·L^{-1}; nano-ZnO-laponite loading amount = 30 g; pH = 7.0; and irradiation time = 60 min).

3.2.3. Effect of UV Wavelength on TCE Removal. With the TCE concentration fixed at 10 mg·L^{-1}, a reaction time of 60 min, a pH of 7, and a nano-ZnO-laponite insertion amount of 30 g, we performed a comparative experiment on the changes in TCE removal ratio with light-source type. These light sources were UVC with a wavelength of 254 nm and UVA with a wavelength of 360 nm. As a reference, we also inserted nano-ZnO-laponite without using any light source and measured the TCE removal efficiency.

Figure 9 shows the removal efficiencies using UVA and UVC without ZnO-laponite, ZnO-laponite only, and UVC with ZnO-laponite. After 60 min of reaction, the respective TCE disposal efficiencies were 21.6, 37.2, 41.9, and 88.6%. In other words, the disposal efficiency can be ordered as UVC with nano-ZnO-laponite > nano-ZnO-laponite > UVC > UVA. Thus, in the removal of TCE from water, the absorption efficiency attributable to nano-ZnO-laponite was higher than the photocatalytic degradation efficiency, while the photocatalytic degradation efficiency with UVC was higher than that with UVA. This indicates that the pores on the surface or in the interior of the nano-ZnO-laponite had better removal performance than the photons generated by UV and that UVC was better at generating photon energy than UVA [21]. The reason for the high performance of the combined UVC and nano-ZnO-laponite system was that the nano-ZnO-laponite particles had high absorption performance, and the photons generated from the UVC light source reacted with ZnO—the photocatalyst on the surface of nano-ZnO-laponite—and generated radical hydroxide, which removed TCE from the water. This result corresponds with that of a study on paracetamol removal by TiO_2-UVC, UVA, and UVC by Yang et al. (2008) [17], in which TiO_2-UVC showed the highest removal ratio of paracetamol in water.

3.2.4. Changes in Removal Properties with Strength of UV Irradiance. In this test, we evaluated the effects of various UV intensities when disposing TCE in water by absorption and photocatalytic reaction (in conjunction with our newly fabricated nano-ZnO-laponite). As shown in the scheme for the test reactor in Figure 2, four UV lamps were affixed to the reactor. This allowed us to evaluate the effects of UV emission by adjusting the number of the lamps to 0, 2, or 4. The strength of the light emitted by one UVC lamp incident on the surface of the quartz tube enclosing the nano-ZnO-laponite was 2.1 mW·cm^{-2}. Therefore, we performed the TCE removal tests with emissions of approximately 0, 4.2, and 8.4 mW·cm^{-2}; the removal efficiencies were then measured to be 41.9, 71.5, and 88.6%, respectively (Figure 10).

Thus, as UV emission increased, the TCE removal efficiency gradually increased, which was also observed with increasing quantity of inserted nano-ZnO-laponite. We can then conclude that if the light energy was properly absorbed, it was effective in generating radical hydroxide and radical superoxide. In general, the disposal efficiency of a photocatalytic reaction has an empirical relation with the amount of UV emission:

$$k_1 \propto I_a, \tag{1}$$

where k_1 is the reaction speed (min^{-1}) and I_a is the UV intensity (mW·cm^{-2}). According to (1), the TCE removal efficiency increased when the photons generated from the UV lamp moved to the photocatalysts on the surface of nano-ZnO-laponite, where enough energy was generated to stop the electron-hole recombination reactions on the surface of ZnO [22].

3.2.5. Effect on pH on Removal Efficiency. A system's pH can act as an important factor to control the absorption of pollutants with respect to the reactivity and reaction rate of ZnO because it affects the surface charge of ZnO and changes the potential of the redox reaction. Therefore, to determine the effects of pH on the photocatalytic reaction for TCE disposal, we examined photooxidation with a TCE concentration of 10 ppm, four UVC lamps, and pH values of

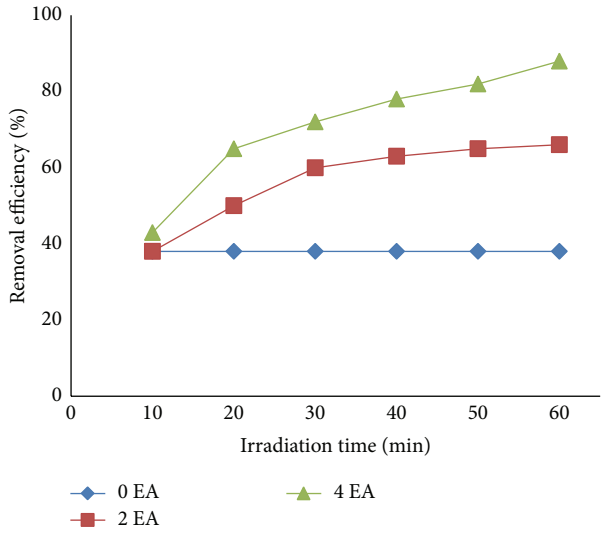

Figure 10: Effect of UVC light intensity on photocatalytic degradation (initial concentration of TCE = 10 mg·L^{-1}; nano-ZnO-laponite loading amount = 30 g; pH = 7.0; irradiation time = 60 min; and UVC intensity = 0–8.4 mW·cm^{-2}).

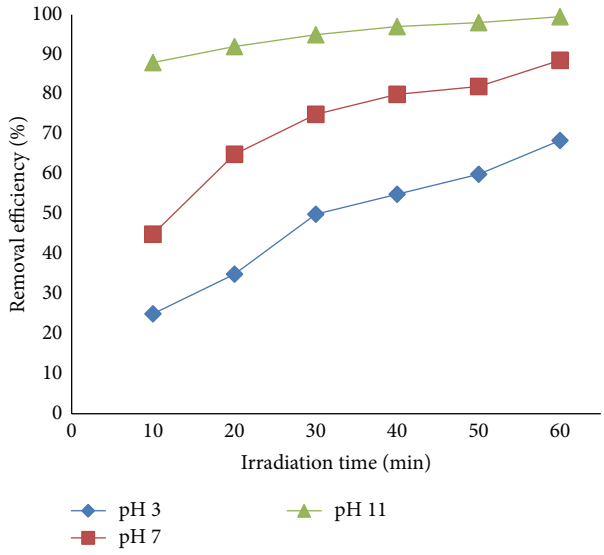

Figure 11: Effect of solution pH on photocatalytic degradation (initial concentration of TCE = 10 mg·L^{-1}; nano-ZnO-laponite loading amount = 30 g; pH = 3.0–11.0; irradiation time = 60 min; and UVC intensity = 8.4 mW·cm^{-2}).

3, 7, and 11; the respective removal efficiencies after 60 min of reaction were 68.5, 88.6, and 99.5% (Figure 11). This means that the removal efficiency was high in the alkaline state but fell lower as the pH value decreased.

It is known that as the pH increased, the activity was improved because the amount of OH^{-1} ions increased on the surface. Therefore, generation of hydroxide radicals increased as a result of the reaction with active OH groups or H_2O on the surface, thus accelerating TCE degradation.

3.3. Consideration. TCE is one of the important nondegradable organic compounds that causes contamination of soil and drinking water. We synthesize a nano-ZnO-laponite complex into ball shape and investigated its TCE removal efficiency under different conditions. In this paper, we try to provide a rather systematic evaluation of the TCE elimination of nano-ZnO-laponite compound under different control parameters, for example, initial TCE concentration, nano-ZnO-laponite amount, UV wavelength, UV irradiance strength, and pH.

And so, nano-ZnO-laponite compound has confirmed the effect of removal of TCE. The mechanisms of TCE removal by using nano-ZnO-laponite compound are two steps, as removal of radical hydroxide that is generated by photons and physically absorbed on Laponite, but each of these two mechanism had not yet been verified. For these two mechanisms, more detailed study and review are necessary.

4. Conclusions

After our investigation on the removal of TCE (a nondegradable substance) using nano-ZnO-laponite balls (a photocatalytic substance), we reached the following conclusions:

(1) While observing whether ZnO crystals were altered by laponite, XRD results for the nano-ZnO-laponite ball showed only particular peaks of ZnO. In the fine-structure analysis, the air-gap ratio of the entire cross-sectional area was found to be 20% or less. Therefore, we can conclude that our nano-ZnO-laponite ball was porous.

(2) The results for measuring the removal efficiency of the initial TCE concentration using UVC showed that decreasing the initial concentration of TCE increased the removal ratio. This occurred because of absorption occurring on the porous surfaces of the nano-ZnO-laponite balls and the generation of hydroxyl ions.

(3) As the amount of inserted nano-ZnO-laponite increased, the TCE removal efficiency increased. The causes were absorption into the porous structures and the constant photocatalytic reactions with increasing quantity of nano-ZnO-laponite balls.

(4) In the examination of the effect of UV wavelength on TCE removal efficiency, the efficiency attained using UVC was found to be about twice that obtained using UVA. This took place because more photon energy was generated at the UVC wavelength (254 nm).

(5) As the irradiance of the UVC lamps increased, the TCE removal efficiency increased. This corresponds with the results of Behnajady et al. [15]: a photon is generated from a free electron in the valence band of the nano-ZnO-laponite ball owing to the change in the electron caused by UV emission.

(6) The TCE removal efficiency was optimal for alkaline values. As the pH increased, the generation of OH radicals increased owing to the reaction with active

OH groups or H_2O on the surface, thus accelerating TCE removal.

Conflict of Interests

The authors declare that there is no conflict of interests regarding the publication of this paper.

Acknowledgment

This study was supported by 2011 Research Grant from Kangwon National University.

References

[1] Y. J. Cho, J. Y. Lee, M. J. Lee, and H. S. Kim, "Cluster analysis of TCE contaminated groundwater," *Journal of the Geological Society of Korea*, vol. 46, no. 1, pp. 49–60, 2010.

[2] Digital Information Center for Environment Research (DICER), "Non-degradable waste water treatment system," *DICER Tech-Info Part II*, vol. 3, no. 7, pp. 278–290, 2004.

[3] C.-H. Kuo and S.-M. Chen, "Ozonation and peroxone oxidation of toluene in aqueous solutions," *Industrial & Engineering Chemistry Research*, vol. 35, no. 11, pp. 3973–3983, 1996.

[4] I. W. C. Lau, P. Wang, and H. H. P. Fang, "Organic removal of anaerobically treated leachate by Fenton Coagulation," *Journal of Environmental Engineering*, vol. 127, no. 7, pp. 666–669, 2001.

[5] W. H. Glaze, J. W. Kang, and D. H. Chapin, "The chemistry of water treatment processes involving ozone, hydrogen peroxide and ultraviolet radiation," *Ozone: Science & Engineering*, vol. 9, no. 4, pp. 335–352, 1987.

[6] C. H. Jeong, "Removal of benzene and toluene by UV photooxidation and photocatalytic oxidatiton," *Journal of the Korea Construction and Environment Association*, vol. 2, no. 4, pp. 117–124, 2003.

[7] S. T. Lee, S. B. Park, and H. M. Oh, *Treatment and Degradation of Hazardous Chlorinated Organic Compounds*, Korea Science and Engineering Foundation, 2003.

[8] K. Y. Kim, *Determination of operational pararmeters for refractory TCE degradation in a photocatalytic oxidative reactor [M.S. thesis]*, Yonsei University, Seoul, Republic of Korea, 1996.

[9] J. Y. Lee and M. H. Koo, "A review of effects of land development and urbanization on groundwater environment," *Journal of the Geological Society of Korea*, vol. 43, no. 4, pp. 517–528, 2007.

[10] B. D. Lee, W. Yoon, and I. H. Seong, "Groundwater quality and contamination characteristics associated with land use in Ulsan area," *Journal of Soil and Groundwater Environment*, vol. 12, no. 6, pp. 78–91, 2007.

[11] A. Fujishima, K. Hashimoto, and T. Watanabe, *TiO_2 Photocatalysis: Fundamentals and Applications*, BKC, Tokyo, Japan, 1999.

[12] M. Kroon, W. L. Vos, and G. H. Wegdam, "Structure and formation of a gel of colloidal disks," *Physical Review E*, vol. 57, pp. 1962–1970, 1998.

[13] M. Morvan, D. Espinat, J. Lambard, and T. Zemb, "Ultrasmall- and small-angle X-ray scattering of smectite clay suspensions," *Colloids and Surfaces A: Physicochemical and Engineering Aspects*, vol. 82, no. 2, pp. 193–203, 1994.

[14] J. O. Fossum, "Physical phenomena in clays," *Physica A: Statistical Mechanics and its Applications*, vol. 270, no. 1, pp. 270–277, 1999.

[15] M. A. Behnajady, N. Modirshahla, and R. Hamzavi, "Kinetic study on photocatalytic degradation of C.I. acid yellow 23 by ZnO photocatalyst," *Journal of Hazardous Materials*, vol. 133, no. 1–3, pp. 226–232, 2006.

[16] H. Yang, G. Li, T. An, Y. Gao, and J. Fu, "Photocatalytic degradation kinetics and mechanism of environmental pharmaceuticals in aqueous suspension of TiO_2: a case of sulfa drugs," *Catalysis Today*, vol. 153, no. 3-4, pp. 200–207, 2010.

[17] L. Yang, L. E. Yu, and M. B. Ray, "Degradation of paracetamol in aqueous solutions by TiO_2 photocatalysis," *Water Research*, vol. 42, no. 13, pp. 3480–3488, 2008.

[18] W. Li, K. Yang, J. Peng, L. Zhang, S. Guo, and H. Xia, "Effects of carbonization temperatures on characteristics of porosity in coconut shell chars and activated carbons derived from carbonized coconut shell chars," *Industrial Crops and Products*, vol. 28, no. 2, pp. 190–198, 2008.

[19] O. Carp, C. L. Huisman, and A. Reller, "Photoinduced reactivity of titanium dioxide," *Progress in Solid State Chemistry*, vol. 32, no. 1-2, pp. 33–177, 2004.

[20] W. K. Choy and W. Chu, "Destruction of o-chloroaniline in UV/TiO_2 reaction with photosensitizing additives," *Industrial & Engineering Chemistry Research*, vol. 44, no. 22, pp. 8184–8189, 2005.

[21] X. van Doorslaer, K. Demeestere, P. M. Heynderickx, H. van Langenhove, and J. Dewulf, "UV-A and UV-C induced photolytic and photocatalytic degradation of aqueous ciprofloxacin and moxifloxacin: reaction kinetics and role of adsorption," *Applied Catalysis B: Environmental*, vol. 101, no. 3-4, pp. 540–547, 2011.

[22] N. Daneshvar, M. Rabbani, N. Modirshahla, and M. A. Behnajady, "Kinetic modeling of photocatalytic degradation of Acid Red 27 in UV/TiO_2 process," *Journal of Photochemistry and Photobiology A: Chemistry*, vol. 168, no. 1-2, pp. 39–45, 2004.